

A Study of the Effect of Surface Metalization on Thermal Conductivity Measurements by the Transient Thermo-Reflectance Method

Mihai G. Burzo
Pavel L. Komarov
Peter E. Raad
e-mail: praad@enr.smu.edu

Department of Mechanical Engineering,
Southern Methodist University,
Dallas, TX 75275-0337

This work is a numerical and experimental investigation of the effect of the use of a metallic absorption layer on the laser-based measurements of the thermal conductivity of dielectric, semiconductor, and highly-conductive materials. The specific experimental studies, which were carried out on silicon dioxide samples, were used to validate the numerical approach and to support the findings of this investigation. The numerical and supporting experimental results reveal the presence of behaviors associated with thermally thin and thermally thick absorption layers, depending on the ratio between the thickness of the absorption layer and the heat penetration depth. It is concluded that the TTR method performs optimally when the thickness of the metalization layer falls in the transition range between the identified thermally thin and thermally thick layers. [DOI: 10.1115/1.1517265]

Keywords: Computational, Electronics, Experimental, Heat Transfer, Thin Films

1 Introduction

The performance of electronic and telecommunication devices depends heavily on electro-thermal interactions, making the knowledge of material properties fundamental to the design process. Higher performance has been achieved by significant reductions in the size of active features as well as by the introduction of innovative materials. Miniaturization leads to increased heat generation densities, which further underscores the importance of thermal analysis. But, in order for the numerical analysis to be useful in the prediction of performance and reliability of integrated circuits, accurate thermal property values are required. With the use of submicron devices came the realization that bulk and thin-film thermal properties differ markedly [1]. However, since no universal behavior is expected for these differences and since they cannot be predicted from theory [2], the properties of each material must be measured separately. Also, as films are typically layered and deposition techniques differ between manufacturers, it is important to measure the interface resistance of stacked layers [3].

There are many experimental techniques [4] that can be used to determine the thermal conductivity of thin-film and multi-layered materials, including the thermal comparator [5,6], embedded electrical resistance bridges [7,8], micro-fabricated thermocouples [9–12], IR thermography [13,14], 3- ω technique [15–17], X-ray reflectivity [18], and ac calorimetry [19–23], among others. However, the transient thermorefectance method (TTR) [24] is preferred among experimental techniques used to determine the thermal conductivity of thin-film and multi-layered materials. The main advantage of the TTR method is that it is a non-contacting and non-destructive optical approach, both for heating a sample under test and for probing the variations of its surface temperature [19]. Because the method is noninvasive, it is attractive for the measurement of the thermal properties of thin-layer materials whose investigation by contact methods would present the diffi-

culties of having to fabricate a measuring device into a sample, and then having to isolate and exclude the influence of that measuring device.

Of course, newly developed materials present an initial hurdle to the TTR method because of the poor availability in the open literature of required material properties. But even when available, TTR measurements of the thermal conductivity can still be hindered by less-than-desirable optical properties of the top layer material (i.e., low thermorefectance coefficient, low reflectivity, high transparency, surface roughness), which degrade the measurement performance of a given system. More specifically, most dielectric materials have a low value of the extinction coefficient, k , which means that they are transparent to the irradiation of a heating laser. If the light penetration depth of the irradiation, $\delta_L = \lambda/4\pi k$, is larger than the layer thickness, h , the laser light cannot heat the layer under test, and thus the TTR method does not work. The next important problem is associated with the value of the thermorefectance coefficient of the top layer material, which defines the rate of change in the reflectivity as a function of the temperature of the sample surface. This coefficient needs to be sufficiently high in order to obtain an appropriate signal-to-noise ratio in the measurements. Usually, it must be higher than 10^{-5} per Kelvin. In addition to the requirement for the thermorefectance coefficient, the range of linear behavior between changes in reflectivity and changes in temperature has to include the range of transient temperatures experienced by the surface during the measurements. Otherwise, nonlinear effects could entirely distort the transient temperature response of a sample during analysis. Another difficulty connected with the optical properties of the top layer is the changing of those properties with time due either to long-term oxidization at room temperature or to accelerated oxidization at the higher temperatures experienced during laser irradiation pulsing. These chemical modifications of the top layer add uncertainty to the measurement procedure since they are not easily quantifiable.

In order to eliminate these difficulties, investigators have resorted to the use of a so-called metal “absorption” layer on top of the material under test (for instance Au in [25], and Al in [3]).

Contributed by the Heat Transfer Division for publication in the JOURNAL OF HEAT TRANSFER. Manuscript received by the Heat Transfer Division December 20, 2001; revision received July 24, 2002. Associate Editor: G. Chen.

Metal films are used because they exhibit high absorptivity and their optical properties are usually well known. Although the use of other metals as an absorption layer has not been widely considered, gold seems to be a particularly attractive material for use as an absorption film because of good stability in its refractive indexes (n and k) in a normal laboratory environment, linear dependence between reflectivity and temperature changes in the range of up to 200 K, and sufficiently high thermorefectance coefficient.

Because of the transient nature of the laser heat source in the TTR method, the duration of a laser pulse and the wavelength of the laser light are essential parameters for analyzing the applicability of the TTR method to a particular situation. Although a number of publications have reported on the use of the TTR method for measuring different composite materials [26], a systematic investigation of the influence of the essential parameters in the TTR method on the uncertainty of the measured thermal conductivity of bulk semi-infinite layer samples has only recently been studied by the authors [27]. The present investigation represents the next step in the complexity spectrum of a sample under test, and is focused on the TTR measurements of samples that have at least two layers, one of which is the absorption layer. This work focuses on the influence of the absorption layer on the performance of the thermal conductivity measurements by analyzing the thermal response of dielectric (SiO_2), semiconductor (Si), and highly-conductive (Diamond) materials to the pulsed heating used in the TTR method. It should be pointed out, however, that the three materials considered in this investigation are representative of a wide variety of other materials for which the results obtained here would be applicable. Also, while the TTR system used in this work has a single pulse width (8.6 ns), the methodology and conclusions are largely applicable to other pulse widths and materials whose thermal behavior is governed by the one-equation Fourier heat model. The values of the thermal conductivity (K) and thermal diffusivity (α) for the materials used are as follows: Au ($K=314 \text{ W/m-K}$, $\alpha=1.27 \times 10^{-4} \text{ m}^2/\text{s}$), Si ($K=148 \text{ W/m-K}$, $\alpha=0.94 \times 10^{-4} \text{ m}^2/\text{s}$), SiO_2 ($K=1.4 \text{ W/m-K}$, $\alpha=4.9 \times 10^{-7} \text{ m}^2/\text{s}$), and diamond ($K=2,000 \text{ W/m-K}$, $\alpha=11.1 \times 10^{-4} \text{ m}^2/\text{s}$).

The motivation for this study arose from the discovery of a special behavior in the course of an experimental investigation of gold-covered SiO_2 samples. This interesting behavior was later confirmed by a thorough numerical analysis for samples of differing thicknesses of SiO_2 and Au. It was suspected that this behavior might be caused by the significant difference between the thermal conductivity of Au and SiO_2 , or in other words, that the thermal behavior is governed by the ratio of the thermal conductivity of the underlying material and the metalization layer. To shed light on this hypothesis, numerical studies were pursued for two underlying materials for which the thermal conductivity ratio would be closer to unity (i.e., Si) and much larger than unity (i.e., Diamond). The studies led to the conclusion that the special behavior exists for any thermal conductivity ratio as will be described in the results section below.

2 Experimental Procedure

The schematic in Fig. 1 depicts the square heating and round probing spots produced by the TTR system in the SMU Sub-micron Electro-Thermal Sciences (SETS) Laboratory (<http://www.engr.smu.edu/sets/>). The source of energy in the TTR method is normally provided by a pulsed laser with short pulse duration. During each pulse, a given volume below the sample surface heats up to a temperature level above ambient due to the laser light energy absorbed into the sample. The heating area is specified by adjusting the pulsing laser aperture and the optics of the system. The depth of the volumetric heating, on the other hand, is determined by the optical penetration depth, which is a function of laser wavelength and surface material properties. The heating energy distribution through the penetration depth (δ_L)

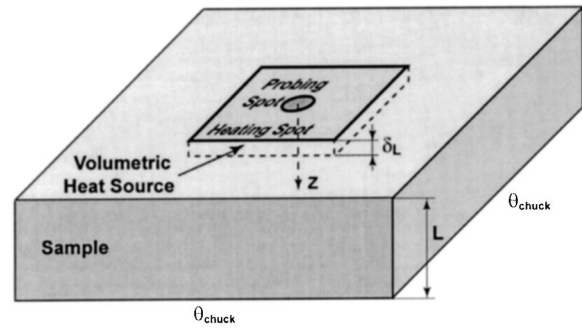


Fig. 1 Schematic of the heating and probing spot positioning on the sample

obeys an exponential decay law, as described later. After each laser pulse is completed, the sample begins to cool down to the initial ambient temperature. During this process, the probing CW laser light reflected from the sample surface at the heating spot center (probing spot on Fig. 1) is collected on a photodetector that reads the instantaneous surface reflectivity. The changes in surface reflectivity are linearly proportional to the changes in surface temperature, within a wide but finite temperature range.

The existing experimental TTR system at the SMU SETS Laboratory is depicted schematically in Fig. 2. The heating source is provided by an Nd:YAG pulsed laser whose wavelength is 532 nm, pulse width is 8.6 ns, and maximum pulse energy is 0.5 mJ. The laser power and output aperture are computer controlled, but the actual energy level delivered by each pulse is also measured by a power meter. The heating spot of the YAG was characterized by CCD imaging and fast photodiode detection, and was found to have good spatial uniformity and a Gaussian temporal distribution, namely:

$$I(t) = \frac{2F}{\tau\sqrt{\pi}} e^{-4(t-t_0/\tau)^2} \quad (1)$$

Here, F is the fluence of laser irradiation, $t_0=9.6 \text{ ns}$ is the time at which the intensity reaches its maximum value, and $\tau=8.6 \text{ ns}$ is the “duration of the laser pulse” (defined as the full-width of the pulse at $1/e$ -height).

The probing light source is an Ar-Ion CW laser with a linearly polarized, single-mode irradiation beam at a wavelength of 488 nm. The beam is delivered to the microscope assembly via a polarization preserving, fiber optic cable with TEM_{00} mode. The microscope objective lens focuses the laser light on the sample surface concentrically with the heated spot. The probing beam reflects from the heated surface back along its optical path to the sensitive area of a pre-amplified silicon PIN photodetector (rise time $\leq 1 \text{ ns}$) through a fiber optic cable. The intensity of the reflected light depends on the reflectivity and temperature of the sample’s surface. The photodetector signal, representing the variations in surface reflectivity, is acquired with an 8-bit resolution via a digital oscilloscope at a rate of 2 Giga-samples per second. Several microscope objective lenses are available, but the one used here is 20X, providing heating and probing spots whose diameters are $226 \mu\text{m}$ and $2.4 \mu\text{m}$, respectively, on the surface of a sample under test. The sample under test is placed on a thermal chuck, capable of maintaining the bottom of the sample at an isothermal condition, in the range of $0\text{--}200^\circ\text{C}$ with increments of 0.1°C . All components are computer interfaced for control and data acquisition.

3 Heat Transfer Model

The governing mathematical equation used to model the transient thermal process in the sample is the heat conduction equation [28]:

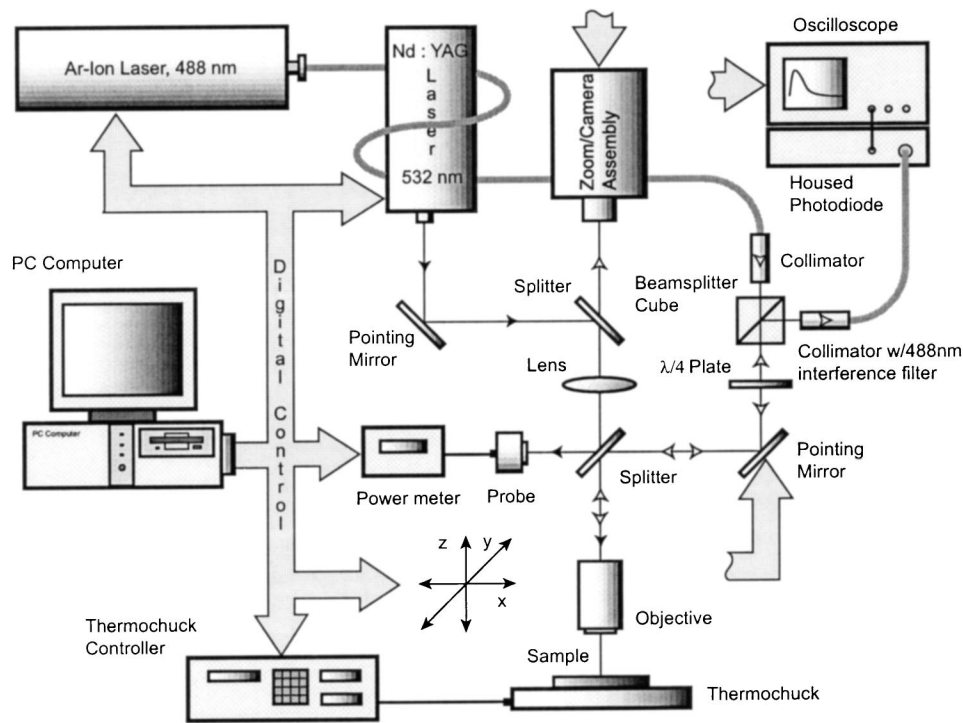


Fig. 2 Schematic of the experimental setup (<http://www.engr.smu.edu/sets1>)

$$\rho C_p \left(\frac{\partial \theta}{\partial t} \right) = \nabla \cdot (K \nabla \theta) + \dot{Q}(r, z, t) \quad (2)$$

where ρ is the material density, C_p is the heat capacity, K is the material thermal conductivity, and \dot{Q} is the heat source term which is a function of radial position, r , depth, z , and time, t . The laser light absorbed by the sample acts as a volumetric heat source, \dot{Q} , such that:

$$\dot{Q}(r, z, t) = I(t)(1 - R)\gamma e^{-\gamma z} \text{Flag}(r) \quad (3)$$

where $I(t)$ is defined by Eq. (1), R is the reflectivity of the top layer, γ is the absorption coefficient of the top layer, and Flag is the heat spot flag, such that:

$$\text{Flag}(r) = \begin{cases} 1 & \text{inside the heating spot} \\ 0 & \text{outside the heating spot} \end{cases} \quad (4)$$

Because of the nature of the problem under consideration (heat spot, structure of the layer, etc.) cylindrical coordinates would normally be preferred. However, since the samples under study are isotropic in the θ -direction, the problem can be reduced to an axially-symmetric, two-dimensional domain. Further simplifications can be obtained by considering that the area of the heat spot is much larger than the probing spot area and that the diameter of the heating laser is much larger than the heat penetration depth, δ_H^* . In such cases, it is possible to solve a much simpler, one-dimensional problem [29,30]. The fact that the problem can be considered one-dimensional has been confirmed by initial computations (the results obtained with one-dimensional and two-dimensional cylindrical coordinates show excellent agreement). The boundary condition at $z=0$ (the upper surface of the sample) is

$$\left(\frac{\partial \theta}{\partial z} \right)_{z=0} = 0 \quad (5)$$

while the boundary condition at $z=\infty$ (the lower surface of the sample) is

$$\theta_{z=\infty} = \theta_{\text{chuck}} \quad (6)$$

where θ_{chuck} is the temperature of the thermochuck and can be adjusted between 0 and 200°C. The initial condition at $t=0$ is

$$\theta_{t=0} = \theta_{\text{ambient}} \quad (7)$$

The heat equation is then discretized by the use of central finite differences for spatial derivatives and a generalized Padé-type differentiation scheme for the time derivative. The Padé based three-point-backward scheme is used because of its higher accuracy and unconditional stability. The resulting algorithm is second-order accurate in both space and time.

Initial computations of the heat penetration depth during the heat transfer process ($\Theta_0 \geq 0.01$), δ_H^* , indicated that the minimum required thickness (measured from the top of the sample) is 26 μm . A fine computational resolution (20 points) inside the smallest characteristic scale of the problem, which is the light penetration depth into the absorption layer, δ_L , requires that the grid size, ΔZ , be 10 Å. In order to estimate the uncertainty of the numerical simulation, a grid convergence study was conducted by obtaining nondimensional temperature responses of a representative problem with different values of ΔZ . The problem consisted of an Si substrate covered with 1 μm of SiO_2 , which in turn was covered with 1.5 μm of Au. The resulting response curves are plotted in Fig. 3 and the maximum error relative to the results obtained with the smallest grid spacing, $\Delta Z = 10$ Å, is shown in the legend for each grid spacing. It can be seen that not only does the temperature response curve converge, but negligible error levels of 0.04 percent are obtained at $\Delta Z = 20$ Å. Therefore, all subsequent computations were conducted with a spatial step size of 10 Å.

4 Results and Discussion

The absorption layer within a substrate is depicted schematically in Fig. 4. Only three length scales are sufficient to uniquely describe the heat transfer problem during pulsed laser heating in the TTR method; namely, the thickness of the absorption layer, h ;

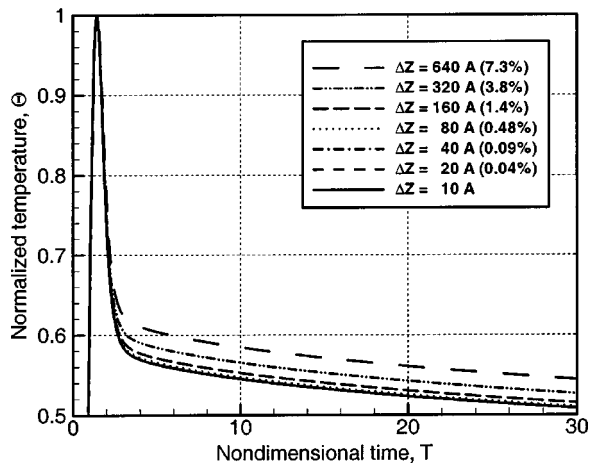


Fig. 3 Uncertainty of the numerical simulation for a Si substrate covered by the $1 \mu\text{m}$ layer of SiO_2 and the $1.5 \mu\text{m}$ layer of Au. Maximum relative errors at the different spatial step ΔZ are shown in the brackets.

the optical penetration depth of the heating light, δ_L ; and the heat penetration depth during the pulse width, δ_H . Since the only absorption layer material considered in the present article is gold, it is reasonable to assume that the heat penetration depth is much bigger than the light penetration depth, i.e., $\delta_H \gg \delta_L$ (this assumption is also applicable to all metals subjected to nanosecond-pulse laser heating). It is equally reasonable to consider that the physical thickness of the absorption layer (e.g., gold) is bigger than the light penetration depth, i.e., $h > \delta_L$. Otherwise, the top layer would be inappropriate for light energy absorption within the scope of the TTR measurement approach. Therefore, if one wishes to analyze the heat transfer process in a gold-covered sample, only two length scales need be considered: h and δ_H . After the introduction of the above reasonable limitations for the geometrical parameters of the problem, one can consider two ranges of variation for h , one larger than δ_H and the other smaller than δ_H . For the former case, when h is larger than δ_H , a practical upper limit must be placed on how thick the gold layer needs to be. To place a practical limit on the required thickness of the gold absorption layer, h^* , it is useful to think in terms of the distance traveled by a heat pulse through the sample until the temperature response falls below ten percent of its maximum value. For the case of gold, h_{Au}^* would be equal to $6.35 \mu\text{m}$ [27].

In the present work, a comparison is made between the temperature responses of two samples of thick SiO_2 , one covered

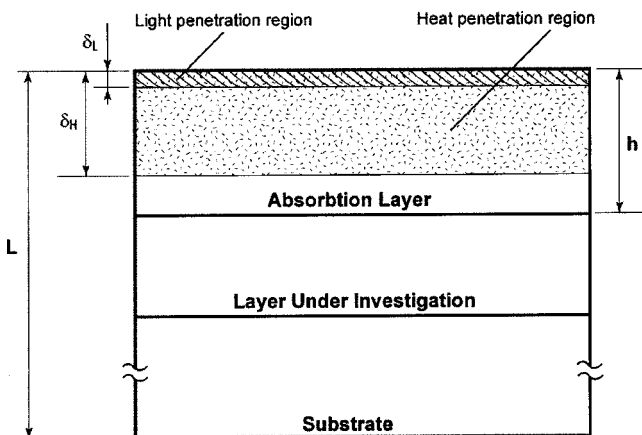


Fig. 4 Schematic of the absorption layer on the substrate

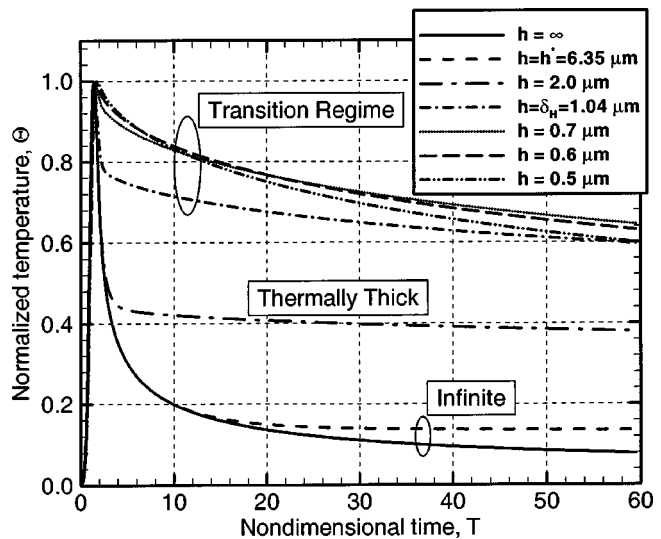


Fig. 5 *Thermally-Thick Layer*: Temperature responses of a SiO_2 bulk sample covered with Au, whose thickness is higher than the heat penetration depth, δ_H

with a (hypothetically) infinite thickness of gold and the other with a layer of gold whose thickness is exactly $h^*=6.35 \mu\text{m}$. The results of this comparison, obtained by numerical simulation, are shown as the lower two curves in Fig. 5. Some discrepancy can be observed between these two curves toward their tail ends, which is due to the influence of the SiO_2 on the heat transfer through the finite gold layer. Nevertheless, it is clear that the gold layer controls the majority of the temporal variations in temperature under the surface of the sample. Thus, the thickness h^* defines the maximum possible thickness of gold to be used as an absorption layer; thicker layers of Au will hide the influence of the thermal properties of any underlying material on the surface temperature response in the TTR method.

4.1 Behavior of Thermally Thick Absorption Layer for SiO_2 . In categorizing the heat transfer process in a layer of material, a distinction is made between layers that are thermally thin and layers that are thermally thick. When the thickness of the absorption layer, h , is larger than the heat penetration depth, δ_H , the layer has sufficient internal thermal resistance to support temperature gradients, i.e., the gold layer behaves as a thick plate. Thus, such a class of absorption layer is referred to as thermally thick.

A typical normalized temperature response for thermally thick layers of gold ($h_{\text{Au}}=2 \mu\text{m}$) is also shown in the middle part of Fig. 5. It is interesting to point out in reference to several of the curves in Fig. 5 that the temperature decay exhibits a sharp change of slope. The slope change corresponds to the time when the heat front reaches the less thermally conductive oxide layer, and is caused by the high temperature gradients developed at the interface between the highly conductive gold layer and the more resistive silicon dioxide layer. As expected, the time required for the heat front to reach the underlying oxide layer is longer for thicker absorption layers. At the upper limit, when the thickness of the absorption layer is bigger than h^* , the response shows that there is very little, if any, heat flow in the silicon dioxide layer, indicating that the bulk limit of the material has been reached.

The preceding discussion dealt with the thermal responses as the thickness of the Au absorption layer was decreased from infinity to $2 \mu\text{m}$. While the curve for $h=\infty$ represents the lower limit for the thermal response at the surface of the sample, the four upper curves in Fig. 5 ($h=0.5, 0.6, 0.7,$ and $1.04 \mu\text{m}$) represent the upper range. Further reductions in the thickness of the gold absorption layer will produce curves that fall below this up-

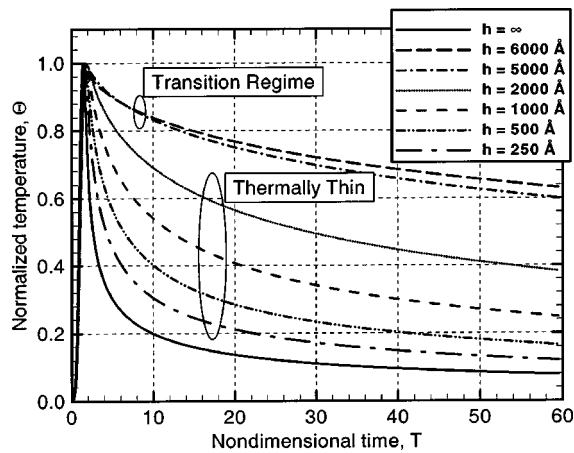


Fig. 6 Thermally-Thin Films: Temperature responses of a SiO₂ bulk sample covered with Au, whose thickness is smaller than the heat penetration depth, δ_H

per range, depicting the behavior of thermally-thin absorption layers. The thermally-thin and transition regimes are discussed next.

4.2 Behavior of Thermally Thin Absorption Layer for SiO₂. When the thickness of the absorption layer is smaller than the heat penetration depth during the heating pulse, the layer has insufficient internal thermal resistance to support temperature gradients, and as a result, the instantaneous temperature field is relatively uniform throughout the material. Consequently, this type of absorption layer will be referred to as a thermally thin (also widely known as “lumped capacity”) layer.

Characteristic temperature responses for thermally thin layers are shown in Fig. 6, bracketed from above by the curve for $h = 0.6 \mu\text{m}$ and from below by the curve for $h = \infty$. The latter curve is included for reference purposes and may not necessarily represent the absolute limit for all materials. The temperature decay is visibly faster as the thickness of the absorption layer decreases and all temperature responses lie above the response for bulk gold. The light penetration depth of the heating laser, δ_L , is the lower limit for the thickness of an absorption layer. Therefore, layers thinner than δ_L are not considered since they are impractical for the TTR method.

4.3 Transition (Intermediate) Regime Limits for SiO₂.

The discussion below can benefit from the use of the Fourier number defined as $Fo = \alpha\tau/h^2$ where α is the thermal diffusivity of gold and τ is the pulse width of the heating laser. It turns out that the reciprocal of the square root of the Fo number (i.e., $Fo^{-1/2}$) represents the ratio between the thickness of the absorption layer, h , and the heat penetration depth during a single laser pulse width, δ_H . The above-defined ratio can also be interpreted as the dimensionless thickness of the absorption layer:

$$H = \frac{h}{\sqrt{\alpha\tau}} = \frac{h}{\delta_H} = \frac{1}{\sqrt{Fo}} \quad (8)$$

The computed normalized temperature responses for gold-covered silicon dioxide are plotted in Fig. 7, where a nondimensional time based on the pulse width has been introduced, such that $T = t/\tau$. In these plots, the temperature responses from Figs. 4 and 5 are shown at specific time instances, beginning with a time equal to twice the pulse width, i.e., $T = 2$, and ending with $T = 50$. This view of the results makes it possible to more easily identify the three different regimes which are entirely defined by the nondimensional thickness H . Behavior consistent with the thermally thick regime appears for $H \geq 2$, while behavior consistent with the thermally thin regime occurs for $H \leq 0.4$. A transition

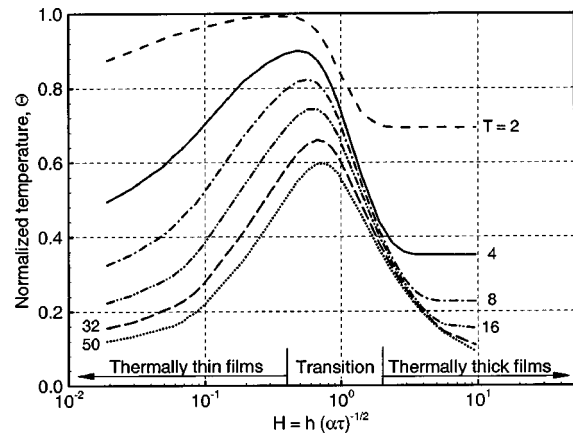


Fig. 7 Heat transfer regimes in gold covered SiO₂ samples

regime between the thermally thin and thermally thick regimes is evident. For the specific materials considered here, this transition occurs in the range of $0.4 \approx H \approx 2$.

Similar numerical experiments were conducted for pulse widths equal to 86 ns and 0.86 ns, thus bracketing by an order of magnitude the 8.6 ns pulse width of the current system. The results (not shown) indicate that the transition occurs in the range of $0.4 \approx H \approx 2$, exactly like for the case of the 8.6 ns pulse width.

The existence of the three regimes defined above was shown for metallized silicon dioxide samples. In the next two sections, the results are presented for Si and diamond, proving that the defined regimes can be identified for materials within a wide range of thermal conductivity.

4.4 Thermal Behavior of Gold-Covered Bulk Si and Bulk Diamond.

The transient surface temperature characteristic of thermally thick and thermally thin layer regimes are presented in Figs. 8 and 9, respectively. The computed normalized temperature responses are plotted in Fig. 10 for different nondimensional time $T = t/\tau$. As previously observed for gold-covered silicon dioxide samples, behavior consistent with the thermally thick regime is evident for $H \geq 2$, while behavior consistent with the thermally thin regime occurs for $H \leq 0.4$. Transition between the thermally thin and thermally thick regimes for the gold-covered silicon sample is clearly visible and occurs again in the range $0.4 \approx H \approx 2$.

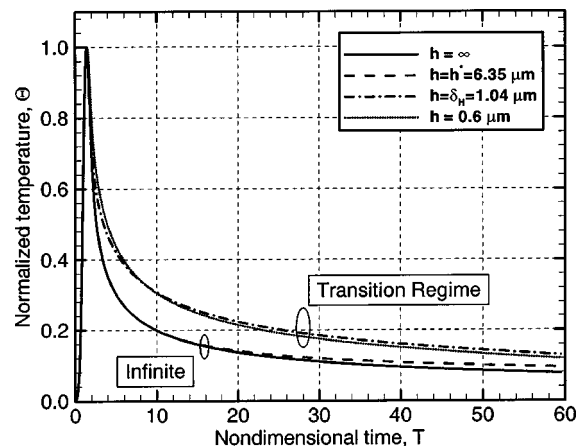


Fig. 8 Thermally-Thick Layer: Temperature responses of a Si bulk sample covered with Au, whose thickness is higher than the heat penetration depth, δ_H

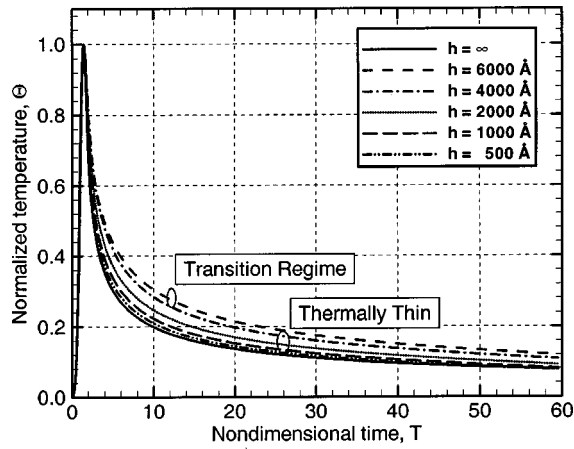


Fig. 9 *Thermally-Thin Films*: Temperature responses of a Si bulk sample covered with Au, whose thickness is smaller than the heat penetration depth, δ_H

Corresponding results for gold-covered diamond are presented in Figs. 11–13. Two major differences from the results shown above for Si and SiO₂ are observed. First, all of the transient surface temperature responses lie below the bulk gold curve (i.e., $h = \infty$). Second, increasing the thickness of Au in the thermally thin regime results in the lowering of the transient temperature

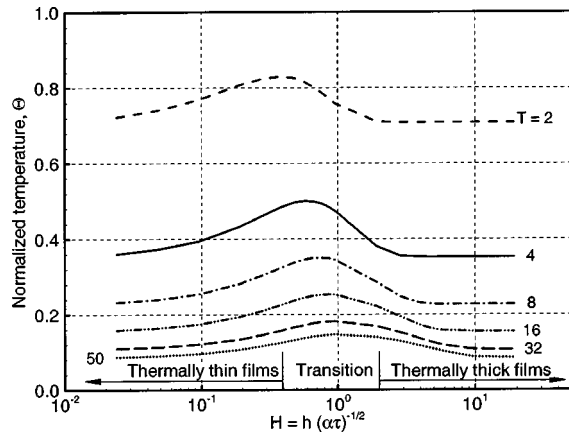


Fig. 10 Heat transfer regimes in gold covered Si samples

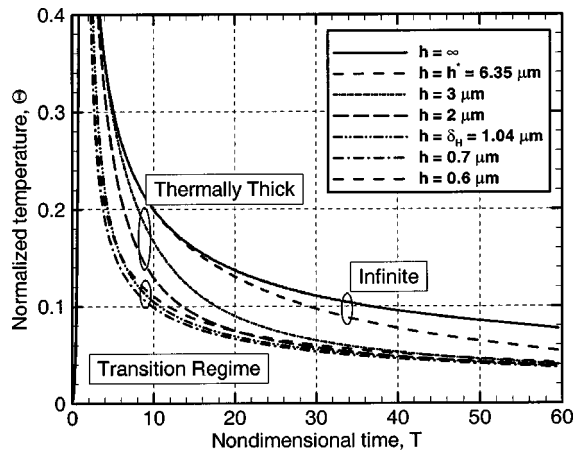


Fig. 11 *Thermally-Thick Layer*: Temperature responses of a diamond bulk sample covered with Au, whose thickness is higher than the heat penetration depth, δ_H

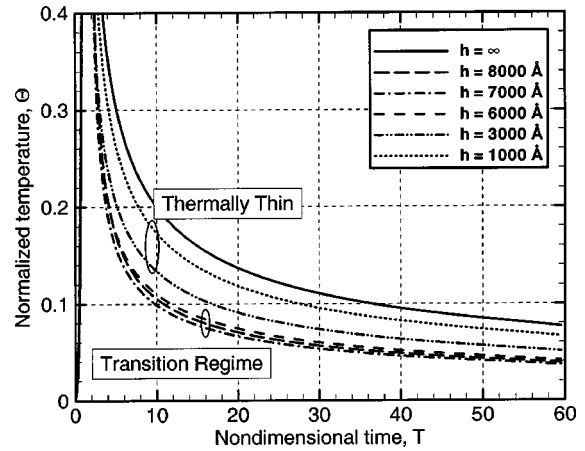


Fig. 12 *Thermally-Thin Films*: Temperature responses of a diamond bulk sample covered with Au, whose thickness is smaller than the heat penetration depth, δ_H

curve, while increasing the thickness of Au in the thermally thick regime results in the raising of the temperature curve. The lowest curve exists in the transition regime. This behavior is the opposite of what was observed in the cases of Si and SiO₂ above. Finally, it should be noted that the behavior observed for gold-covered diamond should be expected for all combinations of underlying material and metalization cover layer whose thermal conductivity ratio is much higher than unity.

4.5 Experimental Results. To validate the temperature response behavior observed in the numerical results presented above for the thin and thick absorption layers, experiments were carried out for different thicknesses of the absorption layer deposited on a given semi-infinite thickness of SiO₂.

In order to determine the minimum required thickness of SiO₂ that behaves thermally as a semi-infinite material, an additional numerical investigation was carried out for seven samples of different thicknesses of SiO₂ covered by 1.5 μm of Au. The results, shown in Fig. 14, indicate that the transient surface temperature response is indistinguishable for layers of SiO₂ thicker than 5000 \AA . Therefore, it was decided to thermally grow 1 μm of SiO₂ on five standard, 4-inch, silicon wafers, and then cover each of them with a metallic layer by a process of chemical vapor deposition. The actual thicknesses of SiO₂ for the five samples were measured with an ellipsometer and found to vary between 1.2 and 1.5 μm , all of which are well above the minimum required 5000 \AA .

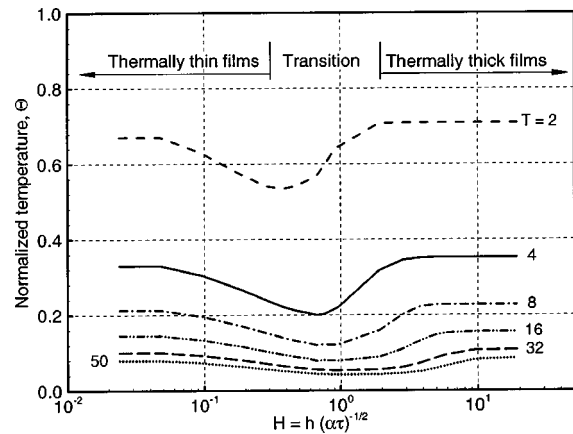


Fig. 13 Heat transfer regimes in gold covered diamond samples

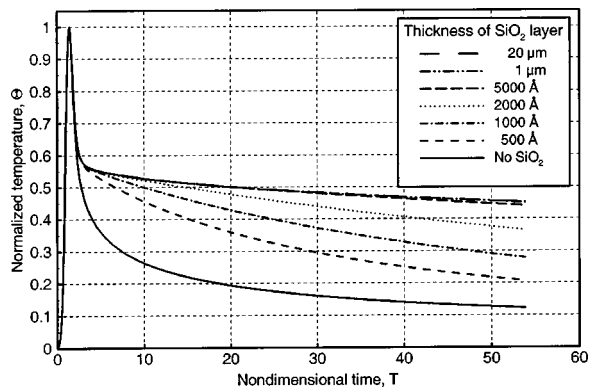


Fig. 14 Influence of the SiO_2 thickness on the normalized temperature response of the gold covered ($h_{\text{Au}} = 1.5 \mu\text{m}$) samples

As previously discussed, the metal of choice for the top layer is gold since gold is chemically stable, has known optical and thermal properties, and has a high thermal reflection coefficient. However, very large thicknesses of gold are inherently difficult and expensive to deposit. Alternatively, a thinner layer of gold was deposited on a thicker layer of aluminum, creating the desired metallic thickness while preserving the advantages of the use of gold as a surface layer. In order to assess the influence of the use of some aluminum in the metallic layer instead of using solely gold, numerical simulations were performed for the scenario of pure gold and a corresponding case of gold on top of aluminum. The simulation results indicated that as expected the differences between the temperature responses for pure gold and gold on aluminum were negligible ($\text{RMS} < 0.6$ percent) since the two metals have similar thermal properties.

The experimental and corresponding numerical results are presented in Fig. 15. The thickness of the coating gold layer for each sample was measured by the use of a stylus profiler with an uncertainty of 5 percent (which is essentially due to the nonuniformity of the coating process rather than the low accuracy of the profiler). The thickness of the absorption layer measured by the profiler is shown in the legend of Fig. 15 for each sample as the sum of the thicknesses of the Au and the Al layers. For each sample, two temperature response curves were obtained numerically in order to bound the variations in the response that would correspond to the 5 percent uncertainty band in the metal thickness. Then, it was found that the experimental data falls within the envelope formed by two response curves. Hence, it became pos-

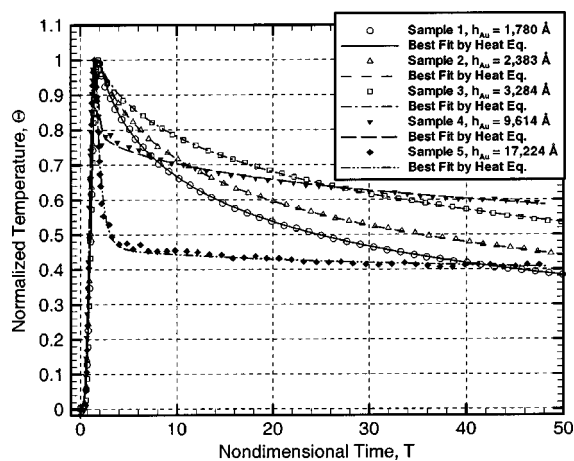


Fig. 15 Measured and computed temperature responses of a SiO_2 layer covered by different thicknesses of gold

sible to select the best fit between the experimental data and numerical curve within the envelope for each curve. The worst average uncertainty in the curve-fitting procedure was equal to 2.2 percent and occurred for Sample 5.

The behavior of the temperature responses of samples 1–3 is consistent with the previously discussed behavior of thermally thin absorption layers (Fig. 15), where the gold layer thickness is considerably smaller than the heat penetration depth during the pulse, and the cooling phase of the temperature response is completely dependent on the thermal properties of SiO_2 . The decrease in the level of the temperature response evident as the gold layer becomes thinner is explained by the fact that the amount of energy accumulated during the pulse decreases accordingly with the reduction of the thermal capacitance of the absorption layer.

Samples 4 and 5 exhibit a behavior consistent with the thermally thick regime whereby the diffusion of heat through the underlying oxide layer is discernable by the presence of an abrupt change of slope at small values of T ($T \approx 2.5$ for sample 4 and $T \approx 3.5$ for sample 5). In this case, both the TTR heating and the beginning of the TTR cooling phases occur within the gold layer, which is highly diffusive for the heat propagation. Thus, the initial decay of the temperature response exhibits a considerable slope, which corresponds to the TTR response of the bulk gold. Contrary to the behavior of the initial decay, the remainder of the temperature response forms a nearly “flat” curve, whose slope corresponds to the slow diffusion of the energy in the SiO_2 medium. This part of the normalized response is lower for thicker layers of gold because the accumulated energy during a pulse dissipates into the gold for thicker gold layers.

4.6 Responsivity of the TTR Method. To further assess the performance of the TTR method, it is useful to introduce a parameter whose value could directly characterize the accuracy of TTR measurements. We suggest the use of the responsivity, R_s , of the thermal conductivity measurement defined as $R_s = K(d\Theta/dK)_{\text{max}}$, where Θ is the normalized temperature response of the sample surface and K is the thermal conductivity of the material. The responsivity R_s is calculated at the nondimensional time Θ where $d\Theta/dK$ is maximum. Indeed, R_s is directly connected with the accuracy of the method by the equation $\sigma_K = R_s^{-1}\sigma_\Theta$, where σ_K is the random measurement uncertainty of the thermal conductivity, K , and σ_Θ is the random apparatus uncertainty related to detecting the temperature response. While σ_Θ depends on the apparatus signal-to-noise ratio and can be considered as a conservative value for a particular setup, the latter equation shows that the measurement uncertainty, σ_K , of the TTR technique decreases with increases in the responsivity value, R_s . Hence, the responsivity, R_s , which depends on the properties and geometry of the materials making up a sample as well as the parameters of the TTR system, can characterize the performance of the TTR method and be useful for optimizing an experiment. By numerically solving the heat equation for Θ , it is possible to compute R_s and to bring out an important issue that could be used to assess the performance of the TTR technique.

The influence of the thickness of the gold absorption layer on the responsivity of the thermal conductivity of three gold-covered samples (silicon, silicon dioxide, and diamond) is shown in Fig. 16. In addition, the responsivity value ($R_s = 0.091$) for an uncovered bulk silicon sample is shown as a dashed horizontal line for reference purposes. For thermally-thick absorption layers, it is expected that the responsivity of the gold-covered silicon sample will be worse than the responsivity of an uncovered silicon sample because a very thick layer of gold will essentially hide the influence of the thermal properties of the underlying silicon material. In the transition and thermally-thin regimes, the responsivity of the gold-covered silicon sample is significantly higher than that of the uncovered silicon sample, except when the thickness of the gold cover becomes smaller than $h_{\text{Au}} = 2,150 \text{ \AA}$ ($H = 0.207$). The improvement is as high as 40 percent at the specific optimal thickness of gold $h_{\text{Au}} = 5,700 \text{ \AA}$, which corresponds to $H = 0.558$.

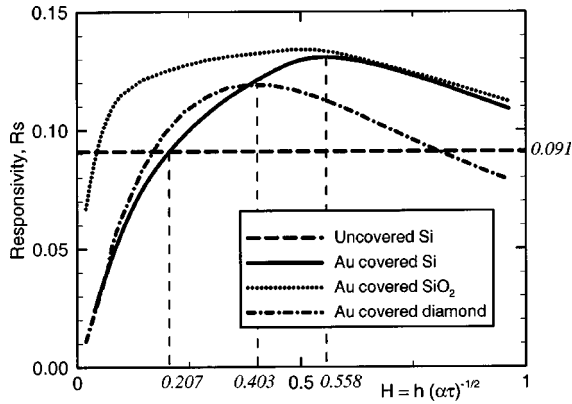


Fig. 16 Influence of thickness of Au absorption layer on the responsivity of thermal conductivity measurements for Si, SiO₂ and diamond samples

Based on this investigation, one can conclude that it is not advisable to use absorption layers that are in the thermally-thin regime (i.e., $H < 0.207$) since these layers result in much lower responsivity values. Furthermore, in attempting to measure lower thicknesses of the absorption layer one can expect to incur higher levels of uncertainty.

By increasing the thickness of the gold layer on an SiO₂ or diamond sample, the responsivity exhibits a similar behavior and noticeably higher R_s values. However, unlike silicon, SiO₂ and diamond are transparent materials; so, if it were not for the presence of the metallic layer, the heating laser would not have been able to heat the SiO₂ and diamond test samples. Therefore, it is impossible to estimate the accuracy gain resulting from the use of a gold cover for an SiO₂ or diamond sample.

4.7 Measurement Uncertainty. As described earlier, the TTR measurement procedure consists of both experimental and numerical parts. The experimental part includes heating the sample under test and detecting a change in the surface reflectivity caused by the temperature change in the heated area, while the numerical part consists of simulating the heat transfer process through the multi-layered sample. Both parts are expected to introduce errors into the respectively obtained normalized transient temperature responses. On the basis of the uncertainty analysis developed by Kline and McClintock [31] and revised later by Holman [32], the average discrepancy between the experimental data and the numerical fitting curve is given by:

$$\sigma_{\text{fit}}^2 = |\sigma_{\text{exp}}^2 + \sigma_{\text{num}}^2| \quad (9)$$

Here σ_{exp} and σ_{num} are the experimental and numerical uncertainties, respectively. Since systematic errors do not exist in the experimental technique, σ_{exp} is tied to the signal-to-noise ratio of the TTR system and can be estimated by calculating the standard deviation of an adequately large number of transient responses. In order to estimate σ_{num} , the responsivity, R_s , introduced in the previous section is used. The responsivity of the normalized transient temperature response for a small relative variation of a parameter V_i of a j -layer of a sample under test is

$$R_{s_{i,j}} = V_i \frac{\partial \Theta}{\partial V_i} \quad (10)$$

where V_i can be one of the following variables: thermal conductivity K , specific heat ρC_p , extinction coefficient k , or thickness of the layer h . Then, assuming that the truncation errors resulting from the discretization of the heat transfer equation are negligible as compared to those associated with the previously listed variables, the uncertainty analysis yields

$$\sigma_{\text{num}}^2 = \sum_i^4 \sum_{\substack{j \neq n \\ \text{if } i=K}}^N (R_{s_{i,j}} \sigma_{i,j})^2 + (R_{s_{K,n}} \sigma_{K,n})^2 \quad (11)$$

Here, $\sigma_{i,j}$ is the relative uncertainty of parameter V_i of the layer j used in the numerical simulation; N is the number of sample layers; n is the particular layer under test; $\sigma_{K,n}$ is the relative uncertainty of the thermal conductivity, K , of the layer under test, n . By substituting σ_{num} into Eq. (9), the uncertainty of the TTR thermal conductivity measurement, $\sigma_{K,n}$, can be re-written as

$$\sigma_{K,n} = R_{s_{K,n}}^{-1} \sigma_{\Theta} = R_{s_{K,n}}^{-1} \left(\sigma_{\text{fit}}^2 + \sigma_{\text{exp}}^2 + \sum_i^4 \sum_{\substack{j \neq n \\ \text{if } i=K}}^N (R_{s_{i,j}} \sigma_{i,j})^2 \right)^{1/2} \quad (12)$$

As evident from Eq. (12), the uncertainty of the measurements $\sigma_{K,n}$ is directly connected to the responsivity R_s . Since the uncertainty σ_{Θ} is an intrinsic parameter of the TTR system, an increase in the responsivity will produce a decrease in the uncertainty of the measurements $\sigma_{K,n}$. Thus, the best uncertainty is obtained for the maximum value of responsivity R_s . Calculating the various terms in Eq. (12) for the present investigation reveals that the total measurement uncertainty is less than 6 percent for the five samples considered.

5 Conclusions

The influence of the thickness of a metallic absorption layer on the performance of the transient thermo-reflectance method has been investigated. The maximum practical thickness of gold that needs to be used as an absorption layer (h^*) was determined, and it was concluded that using thicker layers would hide the influence of the thermal properties of any underlying material. Conversely, the lower limit for the thickness of an absorption layer is the light penetration depth of the heating laser, δ_L , since layers thinner than δ_L do not absorb enough irradiation energy in order to generate the heat source required in the TTR method.

For thicknesses of the absorption layer between the lower and upper limits (i.e., $\delta_L < h < h^*$), the numerically and experimentally obtained transient surface temperature responses differ according to the ratio between the absorption layer thickness, h , and the heat penetration depth, δ_H , during a laser pulse. The two drastically different behaviors are referred to as thermally thick and thermally thin. In the thermally thick regime, a decrease of the absorption layer thickness enhances the normalized temperature response and shortens the time during which the initial rapid temperature decay takes place. In contrast, the normalized temperature response on top of a thermally thin layer exhibits the opposite behavior. Specifically, a decrease of the layer thickness leads to a lower normalized temperature response, but while lower, it remains above the temperature response for bulk gold, even at thicknesses close to δ_L . Between the thermally thick and thermally thin layers there is a range of layer thicknesses where their influence on the temperature response is minimal. The temperature response behavior associated with this range of thicknesses has been referred to as a transition regime.

The analysis performed in the present work has led to the association of the Fourier number (Fo) or the nondimensional thickness of the absorption layer (H) with the different regimes of the normalized temperature response behavior. The thermally thin, thermally thick, and transition regimes have been associated with $H \approx 0.4$, $H \approx 2$, and $0.4 \approx H \approx 2$, respectively.

The responsivity of the TTR measurements characterizes the performance of the TTR method, and makes it possible to recommend optimal thicknesses for a metallic absorption layer. The numerical simulations carried out for the gold-covered Si, SiO₂, and diamond samples revealed that the responsivity values in the thermally thick regime are too low for the measurements to be sufficiently accurate. The same holds true for lower values of H in the thermally thin regime. However, for the range $0.1 \approx H \approx 2$ that

- [24] Tzou, D. Y., 1997, *Macro-to Microscale Heat Transfer (The Lagging Behavior)*, Taylor and Francis, Washington, DC
- [25] Paddock, A., and Eesley, G. L., 1986, "Transient Thermoreflectance From Thin Metal Films," *J. Appl. Phys.*, **60**, pp. 285–290.
- [26] Chen, G., Tien, C.-L., Wu, X., and Smith, J. S., 1994, "Thermal Diffusivity Measurement of GaAs/AlGaAs Thin-Film Structures," *ASME J. Heat Transfer*, **116**, pp. 325–331.
- [27] Komarov, P. L., and Raad, P. E., 2001, "Range of Applicability of the Transient Thermo-reflectance (TTR) Method for Measuring the Thermal Conductivity of Bulk Semi-Infinite Layer Samples," submitted for publication.
- [28] Bejan, A., 1993, *Heat Transfer*, John Wiley and Sons, New York.
- [29] Kading, O. W., Skurk, H., and Goodson, K. E., 1994, "Thermal Conduction in Metallized Silicon-Dioxide Layers on Silicon," *Appl. Phys. Lett.*, **65**, pp. 1629–1631.
- [30] Zhang, X., and Grigoropoulos, C. P., 1994, "The Amplitude Technique for Measurement of Free Standing Thin Film Thermal Properties: A Comparison with other Experimental Techniques," *Proceedings of the ASME Heat Transfer Division, Heat Transfer in Thin Films*, **293**, ASME, New York, pp. 17–24
- [31] Kline, S. J., and McClintock, F. A., 1953, "Describing Uncertainties in Single-Sample Experiments," *Mech. Eng. (Am. Soc. Mech. Eng.)*, January 1953, p. 3.
- [32] Holman, J. P., 1994, *Experimental Methods for Engineers*, sixth edition, McGraw-Hill, pp. 49–65, Chap. 3.